TECHNICAL REPORT • OPEN ACCESS

Beam coupling impedance of the main extraction kickers in the CERN PS

To cite this article: M. Neroni *et al* 2024 *JINST* **19** T08001

View the article online for updates and enhancements.

68th ICFA ADVANCED BEAM DYNAMICS WORKSHOP ON HIGH-INTENSITY AND HIGH-BRIGHTNESS HADRON BEAMS — HB2023

Beam coupling impedance of the main extraction kickers in the CERN PS

M. Neroni [a,b,*] M.J. Barnes,[a] A. Lasheen,[a] A. Mostacci,[b] B. Popovic[c] and C. Vollinger[a]

[a]*CERN,*
Geneva, Switzerland

[b]*Sapienza Università di Roma,*
Rome, Italy

[c]*Argonne National Laboratory,*
IL, United States

E-mail: michela.neroni@cern.ch

ABSTRACT: In view of the High Luminosity (HL) upgrade of the LHC, the beam intensity must be doubled in the injector chain. To perform reliable beam dynamics simulations, the beam coupling impedance in the injectors, such as the Proton Synchrotron (PS), must be followed closely by including all contributing elements into the impedance model. The existing kicker magnets of the PS had been optimized for large kick strength and short rise/fall times, but not necessarily to minimise beam coupling impedance. Hence, unwanted beam induced voltage can build up in their electrical circuits, with an impact on the beam. The beam coupling impedances of the two main kicker magnets used for the fast extraction from PS, the KFA71 and KFA79, are extensively characterized in this study. In particular, electromagnetic simulation results for the longitudinal and transverse coupling impedance are shown. The critical impedance contributions are identified, and their effect on beam stability with a possible mitigation solution is discussed. Moreover, the impact of the cable terminations on the electromagnetic field pattern and possible mitigation techniques are presented, providing a complete impedance evaluation of the entire kicker installation.

*Corresponding author.

https://doi.org/10.1088/1748-0221/19/08/T08001

Contents

1 Introduction

The KFA71 and KFA79 (Kicker Full Aperture) are the fast kickers, together with the septum magnet SMH16 (Septum Magnetic Horizontal) and a set of bumper magnets, involved in the extraction from PS towards SPS (Super Proton Synchrotron) and experimental areas. The extraction kicker system consists of twelve magnet modules which, due to space constraints, were split into two different devices: nine modules are located in a vacuum tank in section 71 (KFA71) and three in section 79 (KFA79) of the PS accelerator. These magnets were first installed in the 1970s [1], and they are nowadays part of the PS multi-turn extraction process, introduced in 2006 to split the beam transversely prior to extraction [2]. In the context of the multi-turn extraction, a measurement campaign of the beam coupling impedance of the PS kickers involved in the process was launched [3]. The impedance of two new kickers, KFA13 and KFA21, which consist of modules similar to those of the PS fast extraction kickers, was measured at that time.

Thereafter, in the framework of the PS machine impedance model and in view of the LHC Injectors Upgrade (LIU), the kickers were identified as the main source of broadband impedance, responsible for the longitudinal loss of Landau damping in the PS [4]. Due to mechanical modifications of the components over the years and due to the high computing resources required to analyse such complex geometries, the beam coupling impedance of the KFA71 and KFA79 was calculated in different iterations with the aim of keeping the PS impedance model updated [5, 6]. The two kicker magnets have been designed for the same functionality, therefore the complete characterization of the beam coupling impedance of the three modules magnet (KFA79) can be used as guiding case also for the nine modules magnet (KFA71). Longitudinal beam coupling impedance calculation results for the KFA79 were presented together with a mitigation solution to reduce the critical impedance contributions [7]. This completed the picture of the longitudinal beam coupling impedance of the KFA79 together with the transverse impedance results, and the study carried out on the nine modules kicker, the KFA71.

The objective of the present work was to present an up-to-date beam coupling impedance model of the PS extraction kickers KFA71 and KFA79, based on the longitudinal and transverse electromagnetic (EM) simulations results. In addition, a possible mitigation solution for reducing the critical impedance contributions in the longitudinal case of the KFA71 is shown here. The influence of the High-Voltage (HV) cables termination on the beam coupling impedance is also introduced and discussed for the KFA79.

2 Electromagnetic calculations

The kickers KFA71 and KFA79 are composed by nine and three modules, respectively. Each module is a 15 Ω delay line consisting of an assembly of nine C-shaped ferrite cells, separated by aluminium alloy laminations (figure 1). Both kicker magnets have a similar layout, with the high voltage connectors of each module facing alternately towards the inside or outside of the PS ring. While the modules of the two kickers have some small differences in their mechanical designs, their assembly remained comparable concerning their EM-features, hence an analogous impedance behaviour is expected.

The EM calculations have been carried out by using the Wakefield solver in CST Studio Suite [8]. Both three dimensional (3D) geometries have been built in CST starting from previous models and by making use of the most recent drawings and CAD projects (figure 2). The three modules kicker, KFA79, is 0.89 m long, and it is assembled inside an octagonal vacuum tank, whereas the nine module magnet, KFA71, is 2.45 m long and it is contained in a cylindrical tank.

These kickers make use of the ferrite material 8C11 [9] which has a dispersive behaviour that was considered by importing measured values of the magnetic permeability as a function of frequency [10]. Due to the high geometrical complexity of the components, the simulation settings were chosen to achieve a compromise between good resolution in the desired frequency range and reasonable computational time.
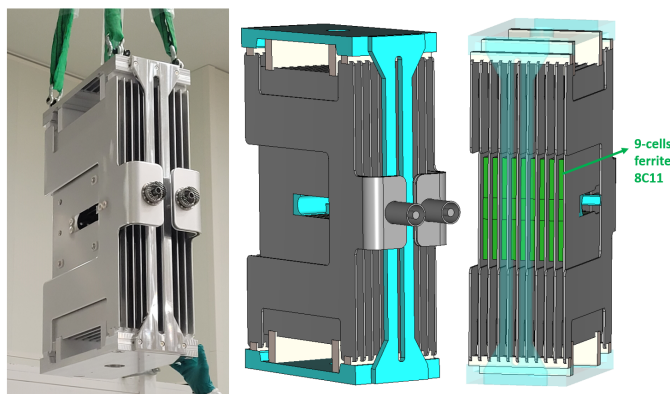
Figure 1. Photo (left) and 3D geometry (right) of a single module of the kicker magnet KFA79, with the assembly of aluminium alloy plates and nine cells of ferrite.
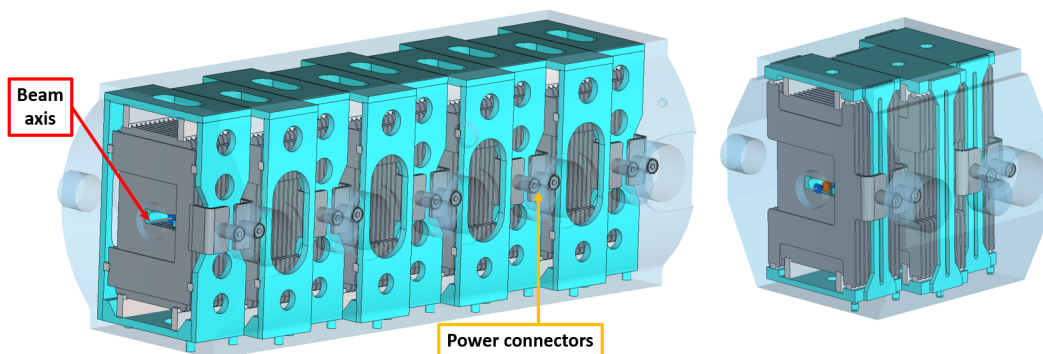
Figure 2. 3D model of the KFA71 (left) and KFA79 (right).
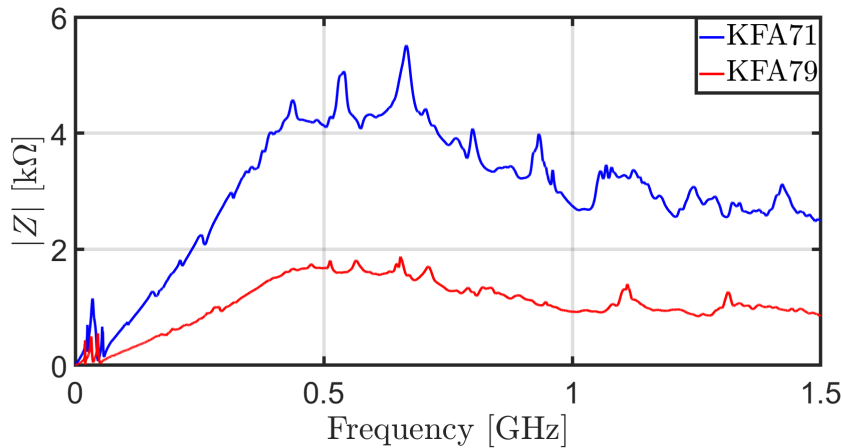
2.1 Longitudinal beam coupling impedance

To calculate the longitudinal beam coupling impedance, a gaussian particle beam with a rms bunch length of 65 mm has been defined in the Wakefield solver. This value was chosen to obtain a good resolution up to 1.5 GHz, the frequency range of the PS beam spectrum. The background material has been considered as the one of the tank walls, stainless steel, with an electrical conductivity of $\sigma = 1.37 \times 10^6$ S/m. Perfect electric boundaries (PEC) have been set in the horizontal and vertical direction, while an open boundary has been selected along the longitudinal beam axis. For the case of longitudinal beam coupling impedance calculation, the wakelength has been selected as sufficiently long to ensure a complete convergence of the wake potential and impedance peaks with saturated amplitude. The main simulation settings are summarized in table 1.

Table 1. Main parameters of CST Wakefield simulations for the longitudinal beam coupling impedance calculation of KFA71 and KFA79.

	KFA71	KFA79
Bunch length rms [mm]	65	65
Wakelength [km]	2	1
Max frequency [GHz]	1.58	1.58
Mesh-cells (hexahedral)	18.9×10^6	19.8×10^6

The impedance of the kickers shows a broadband behaviour, directly proportional to the number of ferrite elements and with a resonant frequency around 600 MHz (figure 3). As expected, with KFA71 containing three times more ferrite elements than the KFA79, the impedance amplitude is three times larger than that of the KFA79. The longitudinal beam coupling impedance of the KFA71 has a maximum amplitude of 5.6 kΩ for a resonant mode at 665 MHz, i.e., at a frequency that is above the main part of the beam spectrum in the PS.

In the low frequency range, up to about 60 MHz, where the beam spectrum is strongest, both kickers show three resonances each (figure 4). In particular, the KFA71 has a resonant mode at

Figure 3. Magnitude of the longitudinal beam coupling impedance for frequency up to 1.5 GHz of both the PS extraction kickers (KFA71 in blue, KFA79 in red).
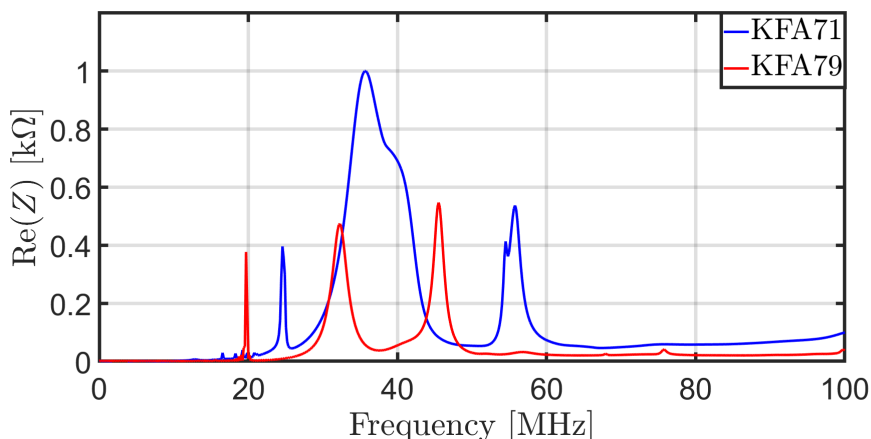
Figure 4. Real longitudinal beam coupling impedance up to 100 MHz (KFA71 in blue, KFA79 in red). Three critical resonant modes are predicted for both kickers.

35.7 MHz with an amplitude of about 1 kΩ. Such large resonances can lead to coupled bunch instabilities [11] and to beam energy losses. It is therefore important to reduce their magnitude, as it will be discussed in section 3.

2.2 Transverse beam coupling impedance

In view of future transverse beam dynamics studies, accurate impedance results at high frequency are needed. Given the high complexity of the kickers' geometry, the best compromise between bunch length, number of mesh cells and wakelength has been chosen. The rms bunch length was reduced to 40 mm in order to increase the frequency range of interest and to obtain an accurate impedance calculation up to 2.5 GHz. In this way, also the tail of the broadband impedance behaviour can be observed.

Both dipolar and quadrupolar component have been computed for the horizontal and vertical directions.

The horizontal and vertical offsets between beam and integration path have been chosen sufficiently small (less than 10% of the dimensions of the rectangular beam aperture, 147 mm and 53 mm respectively), in order to guarantee the validity of the linear approximation of the wake functions [12]. The mesh density has been locally increased in the region of beam and integration path to ensure at least three mesh cells between the two lines. The main simulation settings for the transverse beam coupling impedance calculations are summarized in table 2.

Table 2. Main parameters of CST Wakefield simulations for the transverse beam coupling impedance calculations for KFA71 and KFA79.

$x_{off} = 6.5$ mm, $y_{off} = 2.5$ mm	KFA71	KFA79
Bunch length rms [mm]	40	40
Wakelength [m]	100	300
Max frequency [GHz]	2.5	2.5
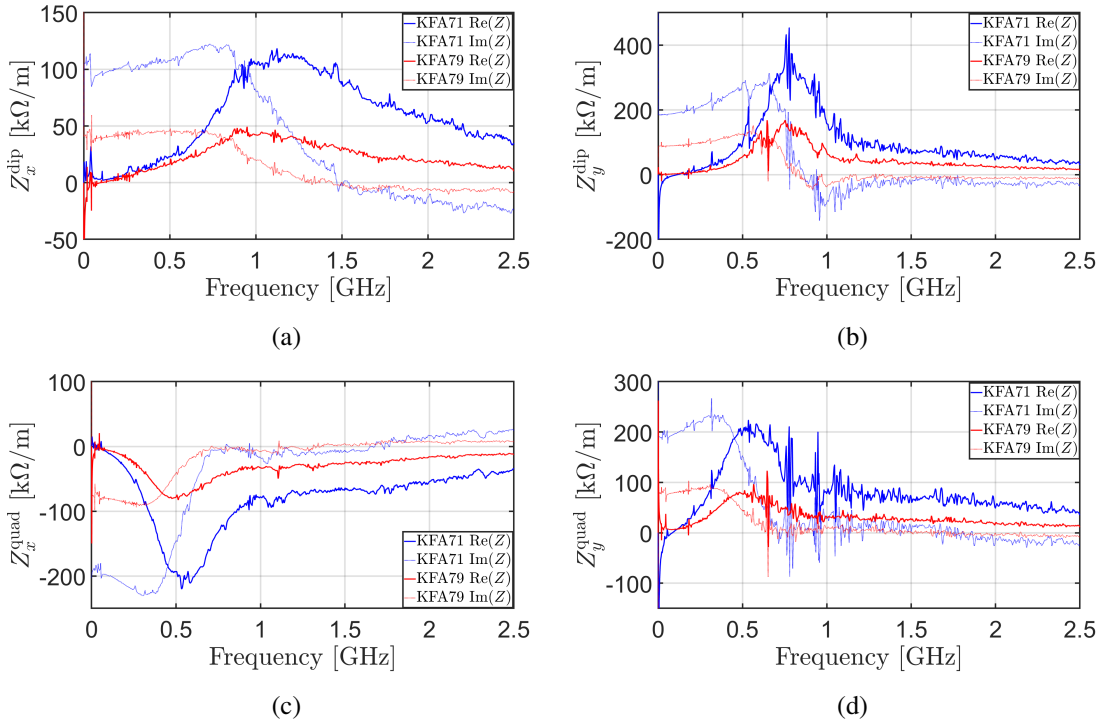
Figure 5. Real and imaginary part of the transverse dipolar horizontal (a) and vertical (b) and quadrupolar horizontal (c) and vertical (d) beam coupling impedance of KFA71 (blue) and KFA79 (red).

The four transverse components were computed by applying the relation [12]:

$$Z_u^{\text{dip/quad}} = -\frac{Z_u(\omega) - Z_u^0(\omega)}{u_{s/t}}. \tag{2.1}$$

The index u takes the values x, y for each of the two transverse planes under consideration, with $x_{s/t}$ and $y_{s/t}$ denoting the horizontal and vertical displacement of the source/test particle, respectively. The parameter $Z_u(\omega)$ is the transverse impedance component computed in CST by shifting either the source or the test particle by a certain offset and $Z_u^0(\omega)$ is the transverse impedance component, which is independent of the particles' offsets. Equation (2.1) is valid under the assumption of absence of coupling between the two planes and a transverse displacement small enough so that second and higher order terms are considered negligible [13].

As predicted by theory, in the case of a rectangular beam pipe [14], the dipolar x and y component differ by about a factor of two (figure 5(a)–5(b)). Moreover, the two quadrupolar components have the same amplitude but opposite sign (figure 5(c)–5(d)).

Focusing on the low frequency range, up to 100 MHz, the horizontal dipolar real component presents strong impedance resonances with a maximum of 32 kΩ/m at 42 MHz. The horizontal and vertical quadrupolar impedances also show strong low frequency resonances, which, in the vertical case, reach up to 37 kΩ/m at 45 MHz. The vertical dipolar component does not present strong resonances at low frequency, however, both the vertical dipolar and quadrupolar impedance show strong oscillations above 700 MHz. In order to better quantify the unwanted modes at low frequency and to exclude simulation artefacts, the simulation should be refined in terms of number of mesh cells and wakelength to obtain an accurate resolution in the frequency range of interest.

Both the real and imaginary parts of the transverse impedances are necessary for transverse dynamics studies to understand their impact on the instability growth rate or betatron frequency spread.

3 Beam impedance mitigation

As anticipated in section 2.1, and according to the analytical estimation in [15], for the PS accelerator, the shunt impedance threshold for driving dipolar or quadrupolar modes, and therefore longitudinal coupled bunch instabilities, is about $R_s \lesssim 2\,\mathrm{k\Omega}$ in the low frequency range ($f \lesssim 40\,\mathrm{MHz}$). This means that any impedance contribution in the low frequency range must be kept to a minimum. The impedance peaks at around $600\,\mathrm{MHz}$ is not object of the present study since, even if they are narrowband resonances, their shunt impedance is well below the instability threshold in the PS.

Focusing on the KFA71, the location of the main high resonant peak, which produces a shunt impedance contribution of $1\,\mathrm{k\Omega}$ at $35.7\,\mathrm{MHz}$, can be identified by looking at the electric field distribution at the frequency of interest. The electric field was calculated from the wakefield simulation by using field monitor at $35.7\,\mathrm{MHz}$ (figure 6).
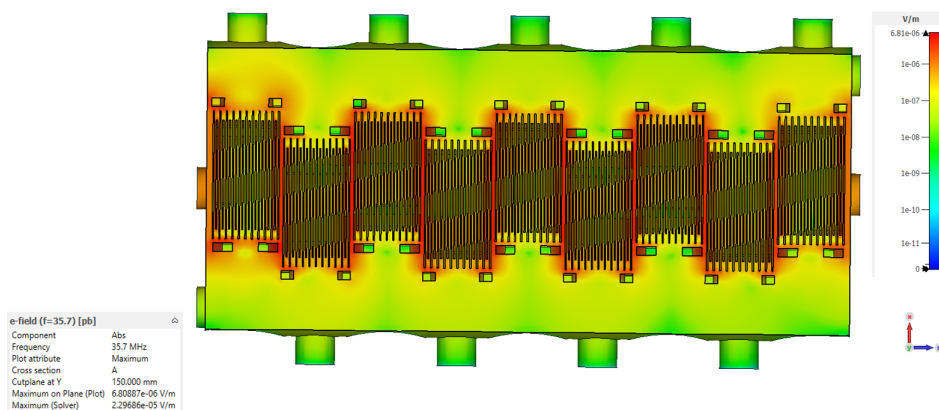

Figure 6. Electric field monitor at $35.7\,\mathrm{MHz}$ in the KFA71. Top view at $150\,\mathrm{mm}$ from the beam axis.

From the E-field monitor it is possible to see a large E-field intensity located between the ground plates of consecutive modules as well as resonances building up between the side walls of the vacuum tank and the ground plates of the modules at the extremities. The E-field monitors at the other two low frequency resonances give a similar result of electric field distribution.

With these results in mind, in order to reduce these critical impedance contributions, the idea is to add conductive bridges that connect all ground contacts. These bridges will provide a path for the currents that are induced in the structure at each beam passage, similar to what has already been proven in the case of the KFA79 [7]. A possible implementation of these transition parts, taking into account the complexity of the structure, is shown in figure 7.

As it is shown in figure 7, the transition parts considered are copper blocks with a shoulder on each side to represent the RF fingers contact. Those have been placed vertically centered with respect to the beam, at a vertical distance of $149\,\mathrm{mm}$ from it, and they are $130\,\mathrm{mm}$ long, the same as the horizontal beam aperture. The KFA71, including the transition parts, was simulated using CST Wakefield solver using a wakelength of $3\,\mathrm{km}$. A comparison of the longitudinal beam coupling impedance of the two cases, with and without the insertion of the transition parts, is shown in figure 8.
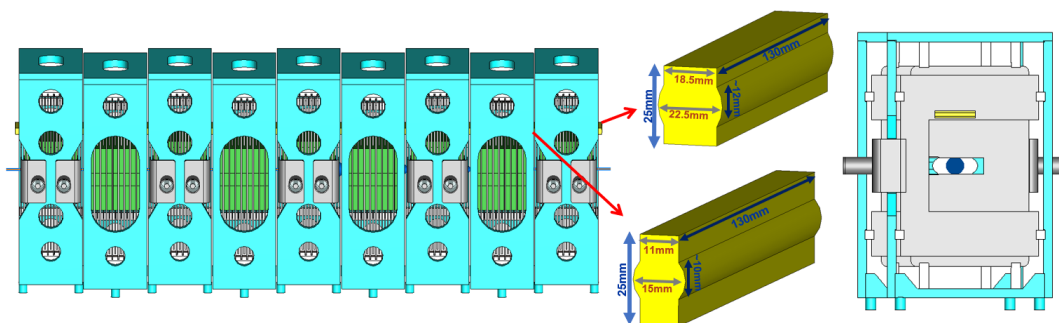
Figure 7. Implementation of transition parts in the KFA71. The copper blocks are inserted between the adjacent modules and between the external modules and the vacuum tank.
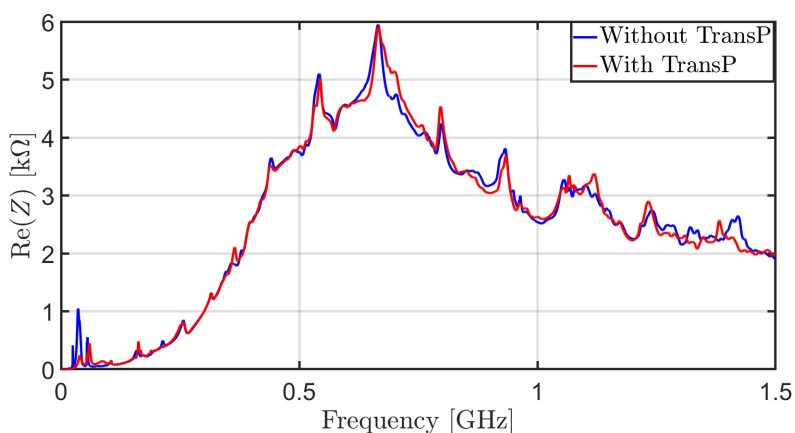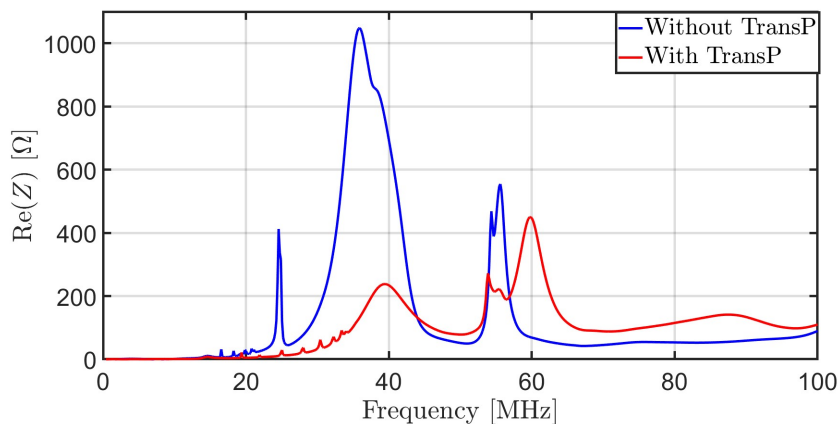

Figure 8. Predicted longitudinal beam coupling impedance of the kicker KFA71 with (red) and without (blue) the inclusion of transition parts. The goal of the transitions is to suppress low frequency resonances without modifying the overall behaviour.

The comparison of the real part of the impedance with and without the mitigation show that the three low frequency peaks are significantly reduced by the inclusion of transition parts (figure 9). This geometrical modification does not affect the broadband behaviour.

As a result, the shunt impedance of the main resonant mode in the low frequency range is five times lower than without the implemented mitigation. The main resonance is now moved to higher frequency, 20 MHz ahead, with a reduced maximum shunt impedance of 400 Ω. The inclusion of a continuity in the ground contacts in the kicker structure would therefore be beneficial in the overall impedance reduction.

4   Impedance calculation including cable terminations

Each kicker module is powered by a high-voltage (HV) pulse generator, connected to the module via two parallel 30 Ω transmission cables. When the module is not being pulsed to extract beam, the main switch thyratron (figure 10) is in the off-state: hence, the main thyratron, end of the transmission cables, presents effectively an open circuit. The output of each module is connected via two parallel 30 Ω

Figure 9. Zoom in the low frequency range of the longitudinal beam coupling impedance of the kicker KFA71 with (red) and without (blue) the inclusion of transition pieces.

transmission cables, to a 15 Ω resistive termination (figure 10). Previous studies point out how the beam coupling impedance response depends strongly on the cables, and how they are terminated [16]. Therefore, it is important to measure and simulate a kicker module in the same configuration as it is in the accelerator, by including all the pulse power connections.
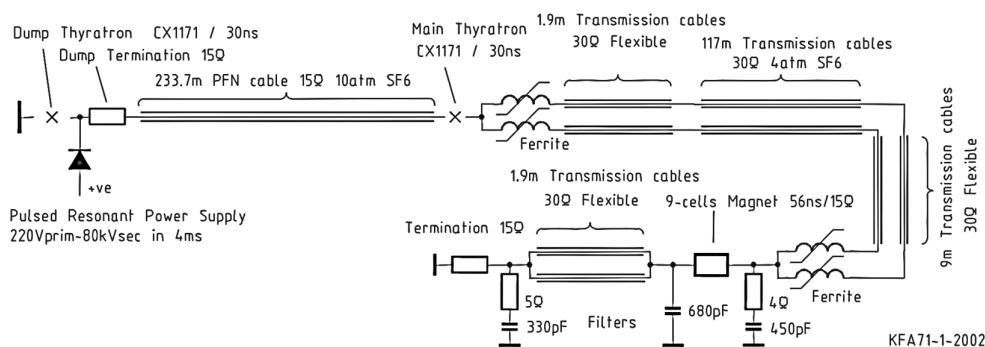
Figure 10. Circuit schematic of a magnet module unit. The output of each module, indicated as "9-cells magnet", is connected to a 15 Ω resistive termination. Reproduced from [17]. CC BY 3.0.

To mimic the measurement setup with a single stretched wire, a simulation of a wire measurement has been carried out in CST. The 3D model includes the full KFA79 kicker, with three modules, a 0.5 mm diameter copper wire positioned at the beam path, and two matching resistors of 220 Ω inserted at the two ends of the stretched wire. The Frequency Domain (FD) solver has been used to compute the scattering parameters. In particular, the transmission parameter, S_{21} is of interest because it directly gives information on the longitudinal beam coupling impedance. The input and output power connectors of each of the three modules have been selected as waveguide ports, this way obtaining an eight ports component.

In CST studio suite, the so-called CST design studio environment allows managing simulation projects, enabling the integration of a lumped element circuit model with a 3D electromagnetic simulation. By using a schematic modelling, the cable terminations could be added to the 3D geometry.
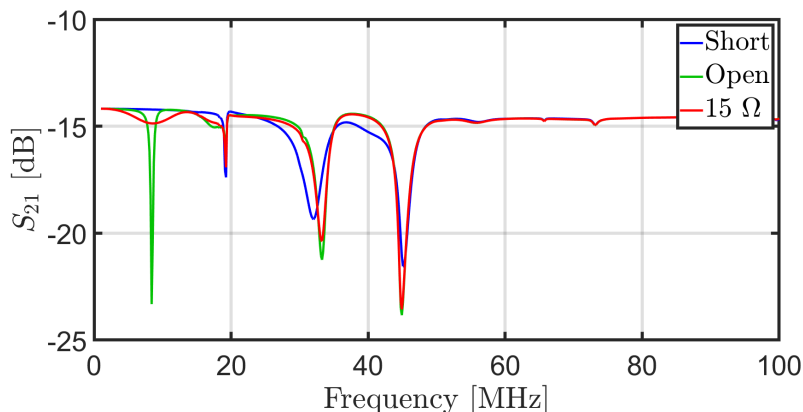
Figure 11. Magnitude of simulated S_{21} parameter versus frequency up to 100 MHz with different electrical cable terminations: short circuit in blue, ideal open transmission line in green and 15 Ω resistor in red.

Different cable terminations have been tested for the output power connectors in order to check their influence on the scattering parameter S_{21}.

Two external ports, at the kicker beam-input and output, were included to excite the structure. For each module, all the input power connectors have been connected to an ideal open transmission line (main switch thyratron in off-state), while the output power connectors have been terminated either with 15 Ω resistors (actual situation), with ideal open transmission lines or with short circuits. The results, for the three cases in the low frequency range, are shown in figure 11. The plotted S_{21} parameter is changed substantially by modifying the cable termination. In particular, in the case of an open transmission line, the scattering parameter presents an additional notch around 8 MHz, while in the other two cases the first notch is at $\sim$ 19 MHz. Hence, the cables and their terminations have a large influence on the longitudinal impedance behaviour in the low frequency range, as they affect the longitudinal beam coupling impedance by shifting the resonant frequency and by changing the amplitude of the modes. Stretched wire measurements on the kicker magnet, including proper cable terminations, are planned to give a final confirmation of these results. As for their impact on the low frequency impedance response, it is crucial to always include the cable terminations, representative of the actual kicker configuration in the PS accelerator, to obtain a realistic impedance model which should be used for beam dynamics studies and instability estimation.

5 Conclusion and outlook

The longitudinal and transverse beam coupling impedances for the two PS extraction kickers, KFA71 and KFA79, have been simulated, and the critical impedance contributions have been discussed. The results will be benchmarked by performing wire measurements to confirm the impedance model. A study of possible mitigation solutions has already started, and the implementation of transition parts between the modules is shown to be beneficial for impedance reduction in the low frequency range. The transverse impedance results are important to update the transverse dynamics simulations with the most recent impedance model. By weighting the transverse impedance with the β-function at the location of the kickers, more information on transverse instabilities can be deduced. Finally, the transmission cable terminations highly influence the beam coupling impedance. Therefore, transmission cables

with their proper terminations should be always included in the simulations and be also part of the measurement setup for obtaining an impedance model representative of the actual kicker configuration.

Acknowledgments

This article is an updated version of the HB 2023 conference proceeding, published under CC BY 3.0 license as [18].

References

[1] D. Fiander, *Hardware for a full aperture kicker system for the CPS*, *IEEE Trans. Nucl. Sci.* **18** (1971) 1022.

[2] M.J. Barnes et al., *The CERN PS multi-turn extraction based on beam splitting in stable islands of transverse phase space: Design report*, CERN-2006-011 (2006) [DOI:10.5170/CERN-2006-011].

[3] E. Métral et al., *Kicker impedance measurements for the future multiturn extraction of the CERN Proton Synchrotron*, *Conf. Proc. C* **060626** (2006) 2919.

[4] M. Migliorati and A. Lasheen, *Plans for tackling the lon- gitudinal instability in PS*, presented at the *9th Impedance Working Group Meeting*, CERN, Geneva, Switzerland, 11 May 2017, https://indico.cern.ch/event/637413.

[5] S. Persichelli, *The beam coupling impedance model of CERN Proton Synchrotron*, Ph.D. thesis, La Sapienza University, Rome, Italy (2015).

[6] B. Popovic and A. Lasheen, *PS longitudinal impedance model*, presented at the *Longitudinal limitations with LIU-PS RF upgrades and mitigation strategy meeting*, CERN, Geneva, Switzerland, 21 September 2018, https://indico.cern.ch/event/750790.

[7] M. Neroni et al., *Characterization of the longitudinal beam coupling impedance and mitigation strategy for the fast extraction kicker KFA79 in the CERN PS*, in the proceedings of the *14th International Particle Accelerators Conference*, Venice, Italy, 7–12 May 2023, pp. 3458–3461 [DOI:10.18429/JACoW-IPAC2023-WEPL150].

[8] *CST Studio Suite*, https://www.3ds.com/products-services/simulia/products/cst-studio-suite/.

[9] Ferroxcube (Data Sheet), https://ferroxcube.home.pl/prod/assets/8c11.pdf.

[10] C. Zannini and G. Rumolo, *EM Simulations in Beam Coupling Impedance Studies: Some Examples of Application*, in the proceedings of the *11th International Computational Accelerator Physics Conference*, Rostock-Warnemünde, Germany, 19–24 August (2012).

[11] A. Lasheen et al., *Identification of impedance sources responsible for longitudinal beam instabilities in the CERN PS*, *CERN Yellow Rep. Conf. Proc.* **9** (2020) 323.

[12] C. Zannini, *Electromagnetic Simulation of CERN accelerator Components and Experimental Applications*, Ph.D. thesis, EPFL, Lausanne, Switzerland (2013).

[13] S. Heifets, A. Wagner and B. Zotter, *Generalized impedances and wakes in asymmetric structures*, Tech. Rep. SLAC/AP110, Stanford Linear Accelerator Center, Stanford University, CA, U.S.A. (1998) [DOI:10.2172/663316].

[14] K. Yokoya, *Resistive wall impedance of beam pipes of general cross-section*, *Part. Accel.* **41** (1993) 221.

[15] E. Shaposhnikova, *Longitudinal stability of the LHC beam in the SPS*, SL-Note-2001-031-HRF, CERN, Geneva, Switzerland (2001).

[16] M. Barnes and L. Sermeus, *Ideas for BE.KFA14L1 Impedance Improvement*, presented at the *27th Impedance Working Group Meeting*, CERN, Geneva, Switzerland, 11 December 2018 https://indico.cern.ch/event/779838/.

[17] L. Sermeus, M. Barnes and T. Fowler, *The Kicker Systems for the PS Multi-turn Extraction*, *Conf. Proc. C* **100523** (2010) WEPD091.

[18] M. Neroni et al., *Beam Coupling Impedance of the Main Extraction Kickers in the CERN PS*, in the proceedings of the *68th ICFA Advanced Beam Dynamics Workshop on High-Intensity and High-Brightness Hadron Beams — HB2023*, CERN, Geneva, Switzerland, 9–13 October 2023 [DOI:10.18429/JACoW-HB2023-TUC4C1].